RSC Advances

PAPER

View Article Online
View Journal | View Issue

Cite this: *RSC Adv.*, 2025, **15**, 30302

Silver–zinc oxide-doped hydroxyapatite nanocomposite: an efficient peroxidase nanozyme for the colorimetric detection of ascorbic acid

Hasib Ullah,[a] Xiaoping Zhang,[b] Wei Sun,[b] Ijaz Ahmad,[a] Imran Rabbani,[c] Khaled Fahmi Fawy,[d] Umar Nishan *[a] and Amir Badshah*[a]

Ascorbic acid is an important player in the food and pharmaceutical industries and plays a key role in the human body. Its abnormal concentration is linked to pathological conditions and monitoring the quality of food and pharmaceutical products. Therefore, it is necessary to monitor its concentration through reliable platforms that are easy to use and affordable. The current work reports a new silver and zinc oxide-doped hydroxyapatite (Ag–ZnO@HAp) nanocomposite based colorimetric sensor prepared using a waste valorization approach through a salt-melting method. The synthesis of the nanocomposite was validated through multiple spectroscopic and morphological techniques, which confirmed the desired synthesis. The synthesized nanozyme was able to act as a peroxidase mimic in the presence of hydrogen peroxide. This activity of the nanozyme resulted in the oxidation of tetramethylbenzidine (TMB) to a blue-green oxTMB. Introduction of the analyte to the system transformed the blue-green color of oxTMB to a colorless form. Various variables affecting the efficiency of the proposed sensor were optimized, and the optimized conditions were reported to be 5 mg of the nanozyme, 4 mM TMB, 18 mM H_2O_2, a pH of 7, and a time of 100 seconds. The proposed sensor showed a significant selectivity towards the specific analyte in the presence of various interfering species. The analytical parameters of the fabricated sensor, such as linear range, limit of detection, and limit of quantification, were reported to be 5–85 μM, 0.5 μM, and 1.6 μM, respectively. The synthesized platform was successfully used for the detection of ascorbic acid in the fruit juices. The synthesized nanozyme has the potential to be used in the food, pharmaceutical, and diagnostic industries.

Received 2nd July 2025
Accepted 11th August 2025

DOI: 10.1039/d5ra04709a

rsc.li/rsc-advances

1 Introduction

Ascorbic acid (vitamin C) is a water-soluble vitamin that is used as an antioxidant in food and beverages.[1] It plays an important role in various metabolic activities in the body. It protects cells from oxidative damage, strengthens the immune system, and prevents a number of diseases, such as the common cold, cancer, and scurvy.[2] It cannot be synthesized by the human body and is obtained from fruits and vegetables.[3] Excess or inadequate amounts of ascorbic acid affect the activities of the human body. Its deficiency can cause scurvy, and an excess amount can lead to hemolysis and kidney stones.[4] Due to its crucial role in the body and use in various industries, it is highly significant to find the accurate amount of ascorbic acid for diagnosis and for monitoring the food quality.

Several traditional techniques have been developed for the sensing and exact measurement of ascorbic acid. They include electrochemistry,[5,6] fluorescence,[7] liquid chromatography,[8] and capillary electrophoresis.[9] Despite the merits of the aforementioned methods, they have some disadvantages. They require costly materials, more time, sophisticated equipment, and complex sample pretreatments.[10] On the other hand, compared with traditional analytical techniques, the colorimetric method has some unique advantages. Colorimetric methods are highly attractive due to their simple operation, cost-effectiveness, high reproducibility, rapidity, and high sensitivity. Furthermore, the results of the colorimetric method can be observed with the naked eye on the spot and can be confirmed accurately by a UV-visible spectrophotometer.

Natural enzymes have been used extensively in colorimetric sensors due to their high catalytic efficiency and specificity. However, several serious drawbacks limit their use in sensing, such as high sensitivity to environmental conditions, a narrow pH range, and low shelf life. Therefore, there is a high demand for alternatives that can function like natural enzymes and

[a]*Department of Chemistry, Kohat University of Science and Technology, Kohat, 26000 KP, Pakistan. E-mail: umarnishan85@gmail.com; amirqau@yahoo.com*

[b]*Hainan International Joint Research Center of Marine Advanced Photoelectric Functional Materials, College of Chemistry and Chemical Engineering, Hainan Normal University, Haikou 571158, P. R. China*

[c]*Department of Pharmacy, Kohat University of Science and Technology, Kohat, 26000 KP, Pakistan*

[d]*Department of Chemistry, Faculty of Science, Research Center for Advanced Materials Science (RCAMS), King Khalid University, AlQuraa, Abha, Saudi Arabia*

overcome the problems posed by them.[11] Nanozymes, *i.e.*, nanomaterials with enzyme-like properties, have attracted much attention because of their enzyme-like profile, robustness, tunable properties, relative ease of synthesis, and stability across a wide range of temperatures and pH compared with natural enzymes.[12] Various materials have been used to mimic the structure and functions of natural enzymes, such as metal oxide, noble metals, and carbon-based nanomaterials. Among metal oxides, zinc oxide leads the pack because of its broad band gap, easy and abundant availability, cost-effectiveness, recyclability, excellent stability, *etc.* However, zinc oxide alone suffers from ineffective use of UV-visible light due to a large band gap of 3.37 eV and rapid hole–electron pair recombination. These shortcomings of zinc oxide can be overcome using various potential noble metals such as Ag, Au, Pt, and Pd. Among these options, Ag offers the best economic viability compared with its counterparts. It decreases the band gap of zinc oxide, increases the electron mobility and imparts new properties to the synthesized nanocomposite. These materials could exhibit catalase-, superoxide dismutase-, oxidase-, and peroxidase-like catalytic activities. Nowadays, peroxidase-like activities of the nanozymes are highly emphasized, occurring in the presence of hydrogen peroxide as an oxidizing agent.[13] However, the nanomaterials used in colorimetric sensing are facing significant challenges of agglomeration and instability, which severely affect their catalytic behavior. In order to overcome agglomeration and retain their catalytic behavior, various matrix materials are used.[14] Materials that are easily available, abundant, biocompatible, and thermally stable are in high demand.[15]

Hydroxyapatite (HAp) is a highly thermally stable, biocompatible, and nanoporous material for the fabrication of nanocomposites that can be used for diverse applications, including sensing. For instance, its use has been reported for the detection of carbon dioxide, glucose, hydrogen peroxide, hydrogen sulfide, cyanide, *etc.*[16] It has some unique properties that make it a prominent candidate for catalyst support. It possesses the capability of ion exchange and high adsorption capacity, which are highly needed for immobilizing active species. It has a nanoporous structure that helps avoid mass transfer limitations. In addition, the weak acid–base properties of HAp reduce the side reactions produced during its use as a supporting material.[17] Different methods have been established for the synthesis of hydroxyapatite.[18] It can be synthesized chemically as well as extracted from bio-wastes such as bones and eggshells.[19] Chemically it can be synthesized from calcium nitrate and hydrogen phosphate.[20] It can also be easily synthesized from natural sources like bovine bone and fish bone.[21] However, naturally derived HAp is preferable due to its lower cost and higher structural biocompatibility.

The present work mainly focuses on the fabrication of silver–zinc oxide-doped hydroxyapatite nanocomposite (Ag–ZnO@-HAp) and its use for the colorimetric detection of the analyte (ascorbic acid). The reported nanocomposite was prepared through a simple calcination method and was used as a mimic enzyme for the selective and sensitive colorimetric detection of ascorbic acid. This strategy offers a highly potent, sensitive, and rapid assay for the detection of ascorbic acid in food quality monitoring and its deficiency-related diseases.

2 Experimental

2.1 Reagents and material

Sodium hydroxide (NaOH), HCl, acetone, disodium hydrogen phosphate (Na_2HPO_4), dihydrogen sodium phosphate (H_2NaPO_4), silver nitrate, zinc acetate, TMB, hydrogen peroxide, and ascorbic acid were purchased from Sigma-Aldrich. Solutions were prepared using deionized water produced in the lab.

2.2 Instrumentation

A UV-visible spectrophotometer, PerkinElmer Shimadzu, Japan, model 1800, was used for recording the spectra of the color change throughout this work. Functional group analysis of the synthesized material was carried out using a Thermo Nicolet, Waltham, MA, model 5700 spectrometer for recording the FTIR spectra of the synthesized material. The range selected for this purpose was 4000 to 400 cm^{-1}. A Gemini 500 (ZEISS, Germany) was used to obtain the scanning electron microscopy images and elemental analysis of the synthesized material. A JEOL (Japan) microscope, model number JEM-2100F, was used to obtain HRTEM images. To determine the crystalline nature of the synthesized material, an AXS D8 X-ray diffractometer was employed. Similarly, an ESCALAB 250Xi (Thermo, USA) was used to analyze the chemical states of various elements present on the surface of the synthesized material.

2.3 Synthesis of HAp and Ag–Zn co-doped HAp

Hydroxyapatite was prepared from waste fish bones *via* the calcination method.[22] Fish bones were collected from a nearby fish point at Kohat bypass, Khyber Pakhtunkhwa, Pakistan. They were first cleaned, washed, and then dried. The waste bones were further treated with 0.1 N sodium hydroxide solution to remove the organic material attached to their surface. They were subsequently treated with acetone for 4 hours to remove the adherent organic moieties. The sample was calcined at 800 °C for 4 hours to obtain white powder. Silver nitrate and zinc acetate (1 : 1) were mixed with hydroxyapatite (1 : 9), respectively. It was further calcined at 800 °C for 3 hours. At the end, a whitish-gray product was obtained and kept for further use.

2.4 Colorimetric detection of ascorbic acid

The detection of the analyte was carried out using the various constituents of the fabricated sensor. For this purpose, a certain amount of mimic enzymes, TMB, H_2O_2, and phosphate buffer saline were used. The detection of ascorbic acid was performed through an indirect mechanism where the blue-green color of oxTMB was transformed to transparent. The reactions were monitored with the naked eye, and confirmation was carried out using a UV-visible spectrophotometer. The sensor system was successfully applied to detect the analyte in fruit juices. To ensure the reproducibility of the results, all the experiments

were performed in triplicate ($n = 3$), and the values are represented as the mean with the standard deviation of the readings.

3 Results and discussion

3.1 Characterization of the synthesized material

The successful synthesis of HAp and Ag–ZnO@HAp was confirmed by FTIR spectra in the range of 4000–400 cm^{-1}, as shown in Fig. 1(a). The major bands around 1100–1000 cm^{-1} and 600–500 cm^{-1} confirm the presence of PO_4^{-3} internal vibrations in hydroxyapatite. These vibrations are due to the asymmetric stretching and bending in the IR region. The peaks around 1400 cm^{-1} indicate the presence of carbonate moieties originating from the remaining organic moieties present in the sample. The peak at 3560 cm^{-1} is attributed to the stretching vibration of the OH^- group in HAp. Owing to the small amount of metals, their peaks are not prominent enough to be indicated here. However, further characterization confirmed their presence.[15,23]

The XRD pattern indicates a crystalline phase with characteristic reflections at Miller indices $2\theta = 25.8$ (002), 28.9 (210), 31.7 (211), 32.1 (112), 32.9 (300), 34 (202), 38 (111), 39.7 (310), 44.2 (200), 46.6 (222), 48.5 (312), 49.4 (213), 50.4 (321), 51.2 (402), and 52 (004) $\pm$ 0.2° in accordance with the JCPDS 09-0432 card.[24] It displays a similar pattern to that of HAp. The presence of these peaks confirms the material's crystallinity and correspondence to the Ag–ZnO@HAp structure. No additional peaks were found in the pattern of XRD for Ag and metal, as such a small percentage of these elements is not achievable under the sensitivity range of the XRD instrument. However, the doping of Ag and ZnO in HAp resulted in peak broadening, as shown in Fig. 1(b), as reported previously in the literature.[25]

XPS analyses were performed to examine the elemental composition and the chemical state of the constituent elements present in the synthesized nanocomposite (Ag–ZnO@HAp), as shown in Fig. 2. Fig. 2(A) shows the expected elements of P 2p, C 1s, Ca 2p, Ag 3d, O 1s, and Zn 2p in the synthesized nanocomposite. The deconvoluted spectrum of carbon (Fig. 2(B)) shows that it is present in three chemical states. The binding energy values of 284.9, 286.2, and 289.2 eV correspond to C–C, C–O, and C=O. Similarly, Fig. 2(C) shows the deconvoluted spectrum of oxygen with binding energy values of 530.9 and 532 eV. These values correspond to oxide ions and absorbed oxygen. The peaks at 347 and 350.7 eV correspond to Ca $2p_{1/2}$ and Ca $2p_{3/2}$, as shown in Fig. 2(D). The binding energy value at 133 eV could be ascribed to P–O in the structure of the synthesized material (Fig. 2(E)). The binding energy values centered at 367.8 and 373.8 eV can be attributed to Ag $3d_{5/2}$ and Ag $3d_{3/2}$, respectively (Fig. 2(F)). The final deconvoluted spectrum, as shown in (Fig. 2(G)), with binding energy values of 1022.2 and 1045 eV, corresponds to the Zn $2p_{3/2}$ and Zn $2p_{1/2}$.[26,27]

The surface morphology of the synthesized material was examined by scanning electron microscopy (SEM) and transmission electron microscopy (TEM), as shown in Fig. 3(A–D). The images (A and B) for pristine HAp showed an irregular spherical shape. Images C and D show the SEM and TEM results of the synthesized Ag–ZnO@HAp, respectively. The morphology depicts a clear doping of the metals on the surface of the HAp matrix. Image E and the inset table show the constituent elements and their percentage composition. As desired, a small amount of the doped elements Zn and Ag was detected. Fig. 3(F–K) shows the elemental mapping of the Ag–ZnO@HAp. These result indicate that the doped elements are uniformly distributed on the surface of HAp. This ensures their availability for catalytic reactions that the current work aims to achieve.

3.2 Colorimetric detection of ascorbic acid

The as-synthesized nanocomposite of Ag–ZnO@HAp was employed as a mimic enzyme for the colorimetric sensing of ascorbic acid. For this purpose, three main reactions were

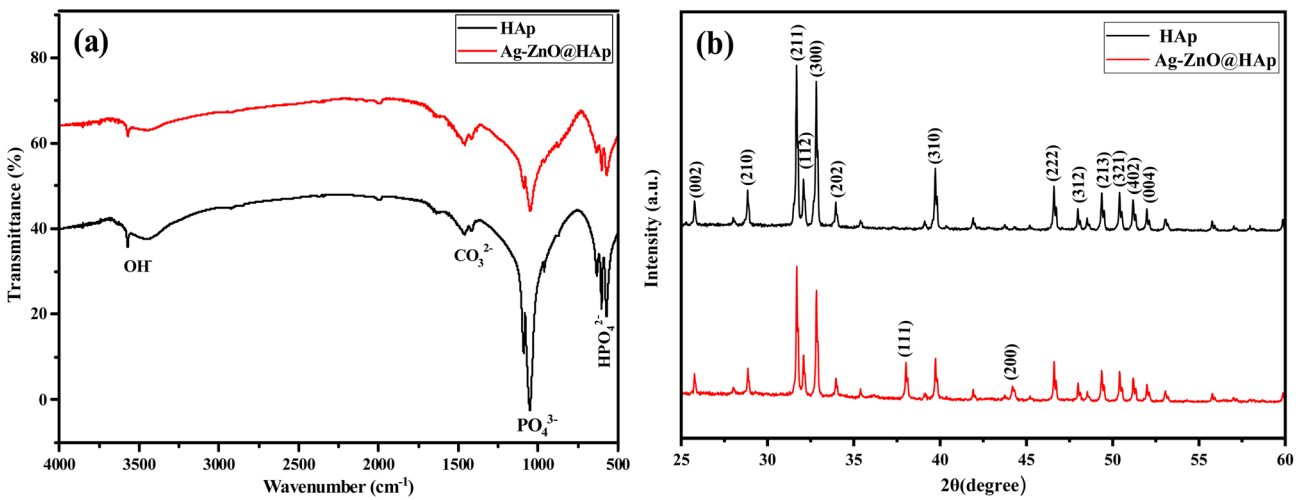

Fig. 1 (a) FTIR spectra of HAp and Ag–ZnO@HAp showing the corresponding peaks of various functional groups present in the synthesized material. (b) XRD spectrogram of the synthesized HAp and Ag–ZnO@HAp showing that the doped material demonstrates peak broadening in comparison to pristine HAp.

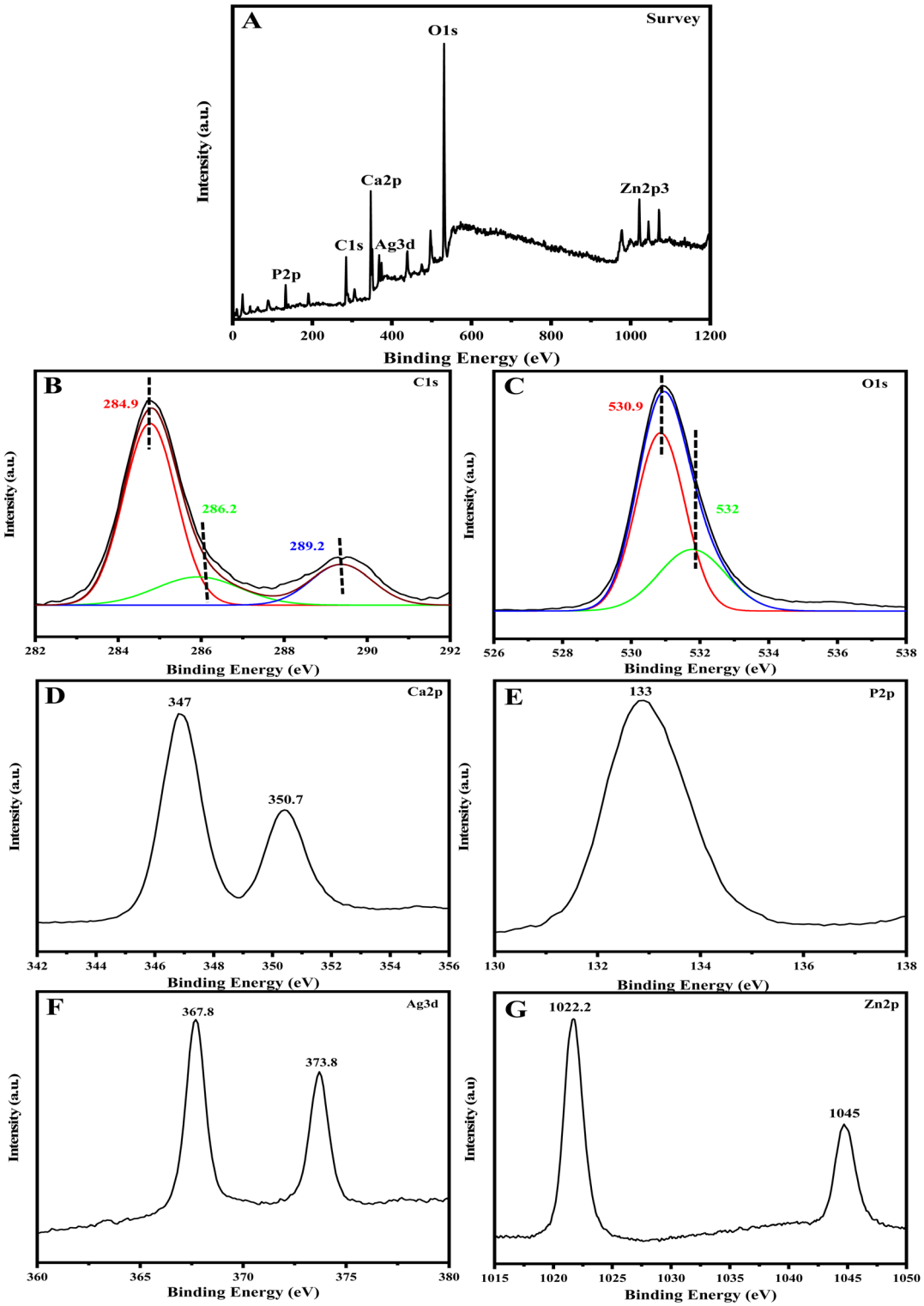

Fig. 2 XPS survey (A) and deconvoluted spectra (B–G) showing the elemental composition and the chemical state of the constituent elements present in the synthesized nanocomposite (Ag–ZnO@HAp).

carried out as, shown in Fig. 4. In the first reaction, represented by curve A, TMB was oxidized with the assistance of hydrogen peroxide. However, this oxidation of TMB was minimal, and a faint blue-green color was observed with the naked eye. It was further confirmed using a UV-Vis spectrophotometer by showing a peak of very low intensity. Upon the addition of a certain amount of the synthesized peroxidase mimic, the color of the reporter dye (TMB) became intense and produced

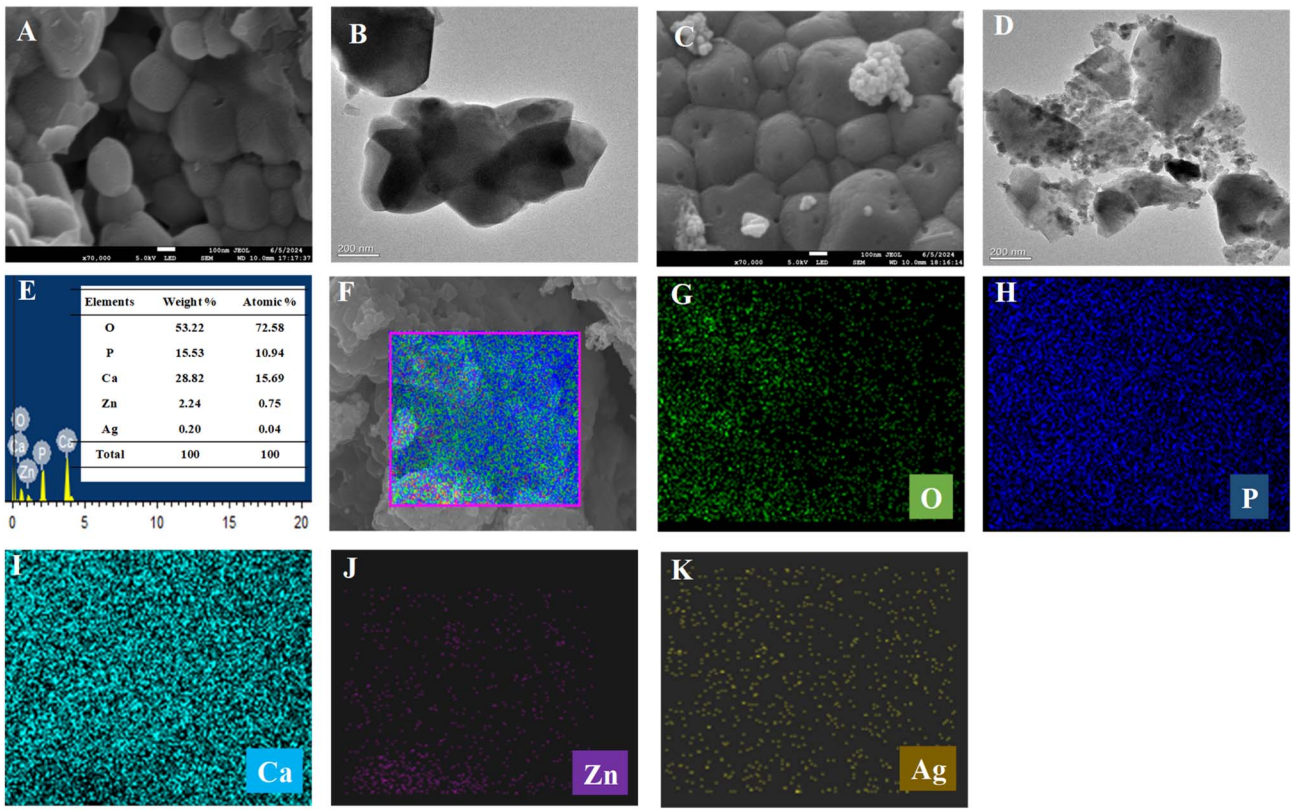

Fig. 3 (A and B) Morphology of the synthesized HAp *via* SEM and TEM. (C and D) Surface morphology of the Ag–ZnO@HAp nanocomposite *via* SEM and TEM. (E and the inset table) Elemental composition and their percentages present in Ag–ZnO@HAp. (F–K) Elemental mapping of the synthesized nanocomposite, showing a uniform distribution of the doped elements.

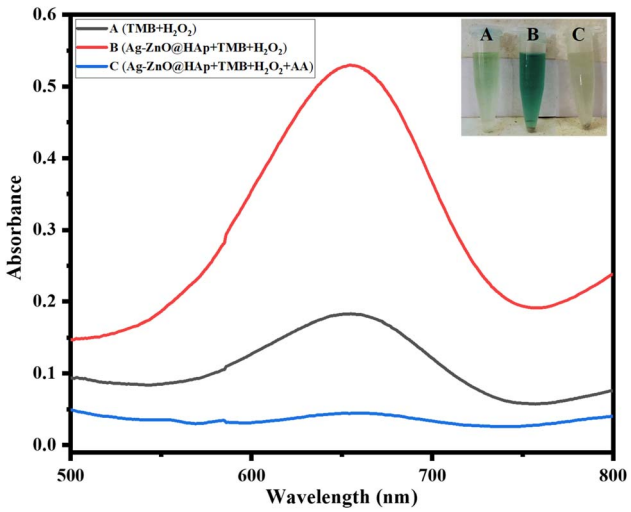

Fig. 4 UV-visible spectra and the colorimetric change (A) in the absence of the nanozyme and (B) in the presence of the synthesized nanozyme. (C) Introduction of the analyte results in the anti-peroxidase-like activity of the synthesized nanozyme, resulting in a change from blue-green to colorless form [the reactions were carried out at neutral pH, with 6 mg of mimic enzyme, 5 mM of TMB, 24 mM of H_2O_2, and an incubation time of 2 minutes]. The corresponding color change has also been represented through inset Eppendorf tubes A–C.

a strong peak at 652 nm in the UV-Vis spectrophotometer, as shown by curve B. At this point, the stage was set for the incorporation of the analyte ascorbic acid (AA). The introduction of the analyte to the sensing platform resulted in the transformation of the color of oxTMB from blue-green to transparent. This visible change was authenticated through UV-Vis spectrophotometry, as shown by curve C.

The performance of the synthesized nanozyme was tested over a period of one month. No significant change was observed in the peroxidase-mimicking activity of the nanozyme, indicating the stability of the synthesized material.

3.3 Proposed mechanism

The sensing mechanism behind the above-mentioned reaction can be elucidated through the proposed mechanism shown in Scheme 1. The peroxidase-like activity of the synthesized mimic enzyme (Ag–ZnO@HAp) results in the generation of hydroxyl free radicals. These radicals attack the TMB and catalyze its oxidation to oxTMB, resulting in a color change from transparent to blue-green. The appearance of blue-green color due to the extensive conjugation is produced by the conversion of the benzoid form to the quinoid form. Due to this increase in conjugation, the gaps between the frontier orbitals decrease, which results in a transition in the visible region, which in this case is blue-green with a peak at 652 nm, in accordance with the reported literature.[15,25] This optical change sets the platform for the sensing of the analyte. When the analyte is introduced into the sensing system, it results in the oxidation of ascorbic acid to dehydroascorbic acid with the reduction of TMB from its

oxidized form. This change in TMB from its oxidized form results in a color change from blue-green to transparent. The optical change was confirmed through a UV-visible spectrophotometer and was also visible to the naked eye. To ensure the production of hydroxyl free radicals during the reaction, different types of radical scavengers, such as *t*-butanol and thiourea, were used. The addition of scavengers resulted in no change in the color of TMB, which chemically confirmed the production of hydroxyl free radicals.[28]

3.4 Optimization of various parameters

The proposed sensing system is dependent on various variables, such as the amount of the mimic enzyme, pH of the sensing system, time, TMB, and H_2O_2 concentration. For this purpose, using the standard procedure of analytical chemistry, one parameter was varied while keeping the others constant. In this way, all the different parameters were optimized before using the sensing system for quantification of the analyte.

Different amounts of the mimic enzyme in the range of 1–8 mg were used to ascertain the optimal amount for the sensing of the analyte, as shown in Fig. 5(i). The best response was obtained at 5 mg, and this amount was used for subsequent reactions. pH is another important factor that affects the performance of a sensor. For this purpose, the proposed sensor performance was optimized in the range of 3–10, with the best response achieved at pH 7, as shown in Fig. 5(ii). The chromogenic substrate TMB was studied in the range of 1–7 mM, and the best response was achieved at 4 mM (Fig. 5(iii)). Hence, this amount of TMB was used for further studies with the proposed sensor. Hydrogen peroxide is another important parameter for the proposed sensor. Different concentrations of hydrogen peroxide in the range of 1–36 mM were studied, and the best results were achieved at 18 mM (Fig. 5(iv)). Response time is another important parameter for examining the performance of the proposed sensor. The sensor was incubated for its best performance, as shown in Fig. 5(v). The result shows a very rapid response in just 100 seconds. After this time, no visible change was observed. Thus, the optimal time was 100 seconds.

3.5 Analytical performance of the fabricated sensor

To authenticate the performance of the fabricated sensor, the quantitative aspects were studied. Ascorbic acid solutions of different concentrations were prepared and tested with the synthesized nanocomposite (Ag–ZnO@HAp). The fabricated sensor detected ascorbic acid over a wide range of concentrations. However, the response of the fabricated sensor was linear in the range of 5–85 μM, as shown in Fig. 6(i) and (ii). The regression coefficient for the linear range was calculated to be 0.9914, indicating the accuracy and precision of the proposed sensor. This indicates that the proposed fabricated sensor can determine the concentration of the analyte in the given range linearly with an acceptable error. Other key parameters, such as the limit of detection (3σ/slope) and the limit of quantification (10σ/slope), were calculated to be 0.5 μM and 1.6 μM, respectively. Here, σ represents the standard deviation of the blank, which signifies the noise or variability in the system when the analyte is not present. The slope represents the ratio of absorbance to concentration, reflecting the sensitivity of the method. These results show that the sensing platform could successfully detect the analyte over a wide range. Additionally, the sensing platform was compared to the previously reported colorimetric

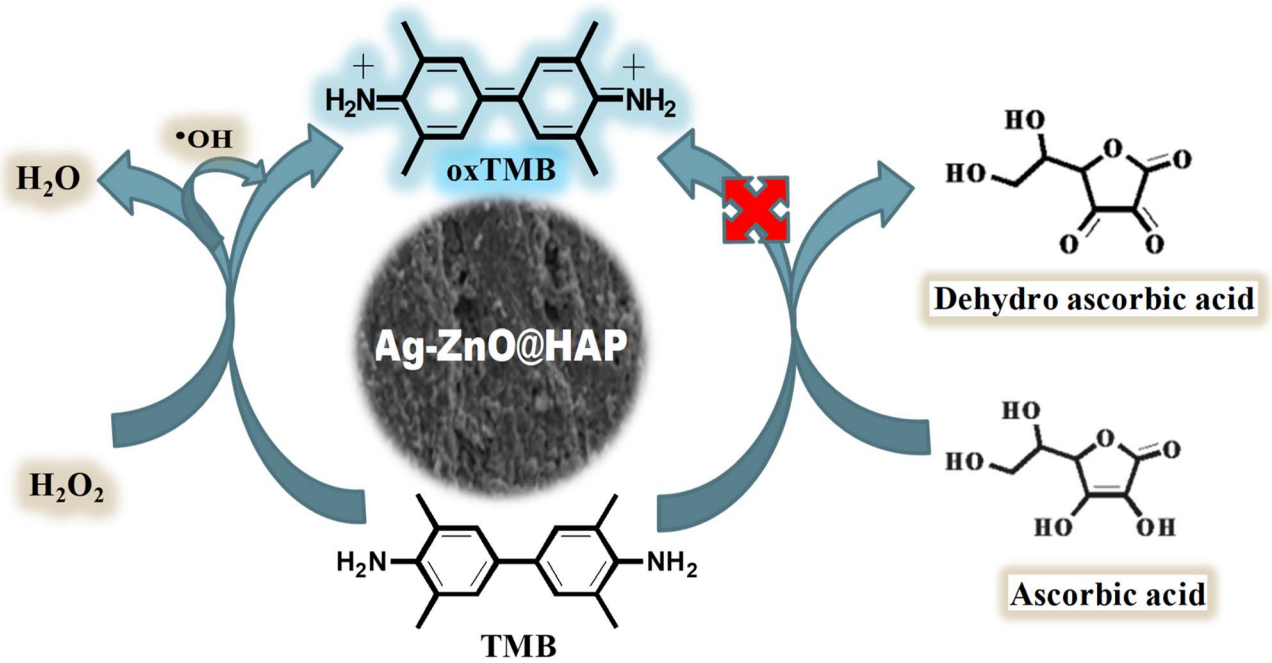

Scheme 1 Proposed mechanism for the colorimetric sensing of ascorbic acid using the Ag–ZnO@HAp mimic enzyme.

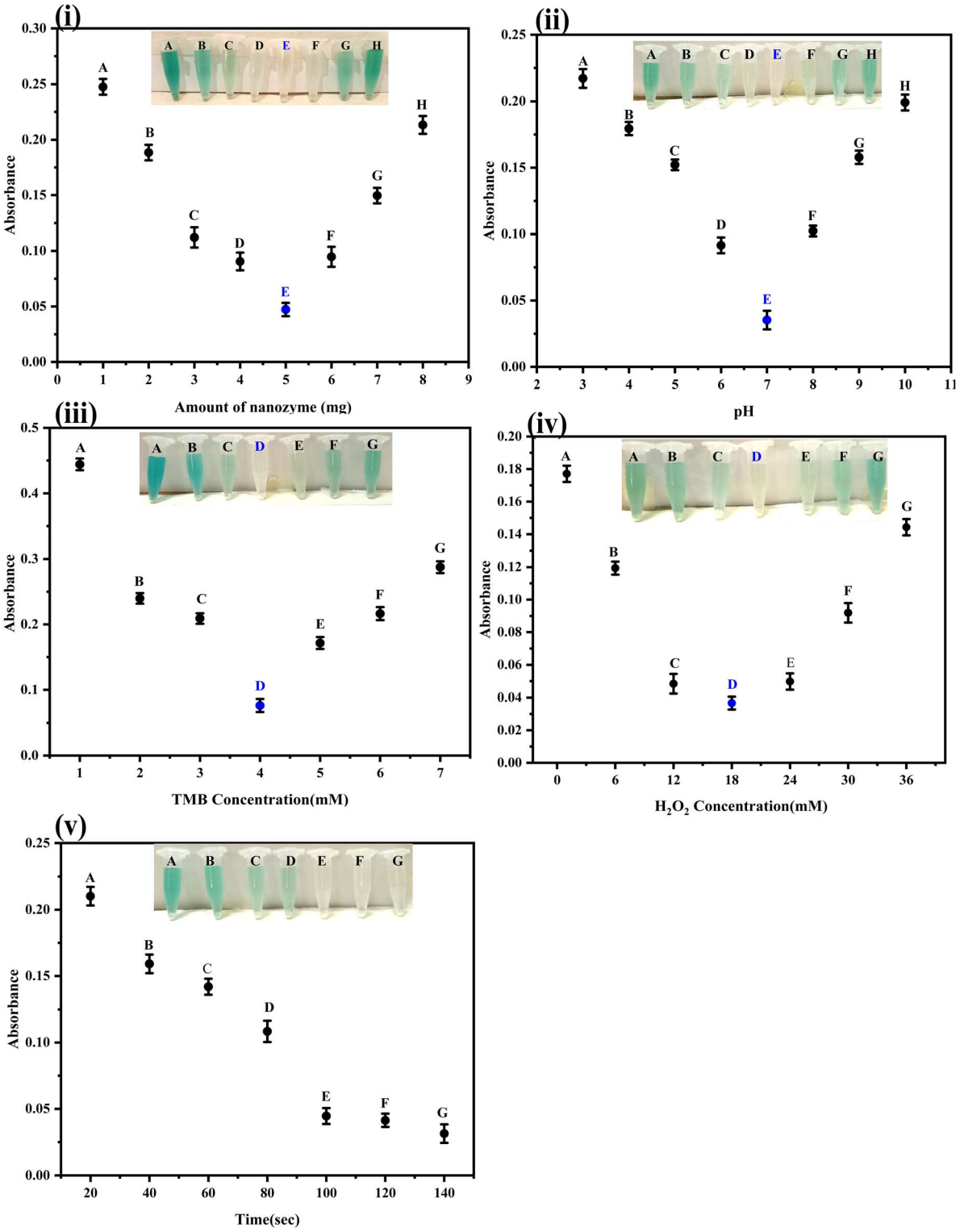

Fig. 5 Optimization study of various parameters including the inset Eppendorf tubes for the respective experiments. (i) Optimization study of the amount of nanozyme, indicating the best performance at 5 mg. (ii) Effect of pH on the response of the fabricated sensor, showing the best response at pH 7. (iii) Effect of TMB concentration, demonstrating the best results at 4 mM. (iv) Effect of concentration of H_2O_2, with the best performance achieved at 18 mM. (v) Effect of time on colorimetric change, showing the best result at 100 seconds [reaction conditions: 5 mg of mimic enzyme, 4 mM of TMB (200 μL), 18 mM of H_2O_2 (200 μL), PBS buffer of pH 7 (250 μL), 85 μM of 100 μL ascorbic acid, and incubation time of 100 seconds ($n = 3$)].

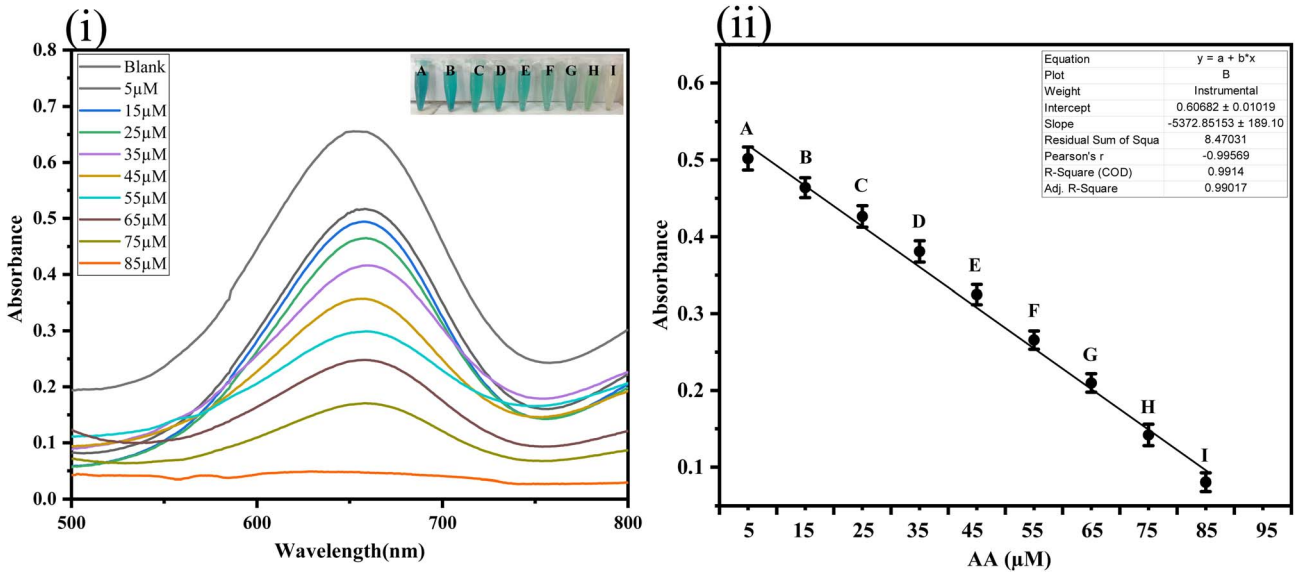

Fig. 6 Analytical performance of the sensing platform represented by the corresponding inset Eppendorf tubes. (i) UV-visible results of the analyte concentrations in the range of 5–85 μM with a linear change in absorbance. (ii) Quantitative relationship between the concentration of ascorbic acid and absorbance ($n = 3$).

Table 1 Comparison of the linear range and limit of detection of different peroxidase-mimicking nanocomposites

Catalyst	Sensor type	Linear range (μM)	LOD (μM)	Reference
PTCA-$ZnFe_2O_4$	Colorimetric	1–10	0.834	29
Pt-HMCNs	Colorimetric	6–60	3.29	30
Co_3O_4@β-CD NPs	Colorimetric	10–60	1.09	31
$AgFKZSiW_{12}$@PPy	Colorimetric	1–80	2.7	32
FeMnzyme	Colorimetric	8–56	0.88	33
FeCo NPs	Colorimetric	0.5–28	0.38	32
Ag–ZnO@HAp	Colorimetric	5–85	0.5	Present work

sensors, as shown in Table 1. The results indicate that the proposed sensing platform has a wide linear range and a low limit of detection.

3.6 Interference study

One of the vital aspects of any sensor is its selectivity. The proposed sensor selectivity was tested in the presence of various interfering species, such as dopamine, calcium ions, glycine, tyrosine, glucose, uric acid, and oxalic acid, under the above-mentioned optimum conditions. As shown in Fig. 7, the analyte exhibited the highest transmittance, while the potential interfering species exhibited the lowest transmittance, indicating approximately no response under the given optimum conditions. Hence, the sensor is highly selective for ascorbic acid detection under the given conditions. It is noteworthy that all the potential interfering species and the analyte were taken at equimolar concentrations (85 μM of 100 μL) for better comparison.

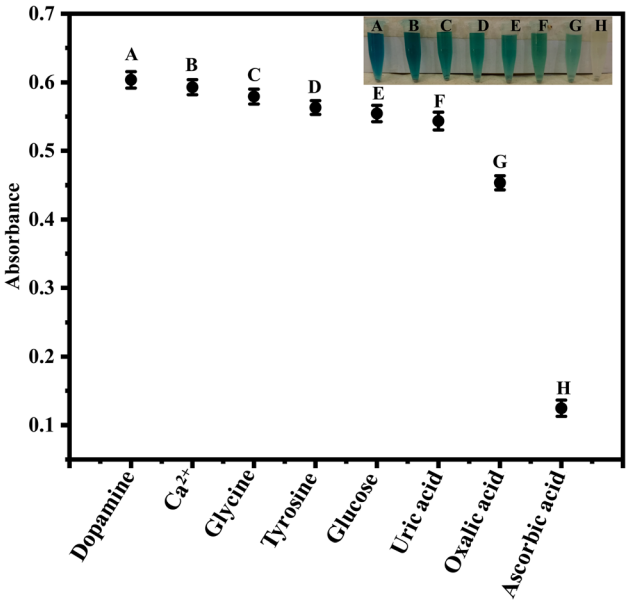

Fig. 7 Interference study of different potential interfering species in the presence of ascorbic acid alongside the inset Eppendorf tubes under optimum conditions. The results explicitly indicate that the proposed sensor is highly selective towards ascorbic acid ($n = 3$).

3.7 Real sample application

The fabricated sensor was successfully applied to detect the analyte in the linear range of the proposed sensor, as shown in

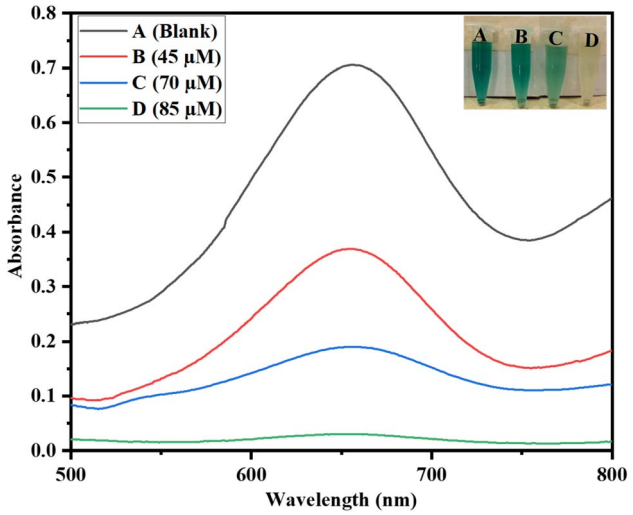

Fig. 8 Real sample application of the proposed sensor alongside the inset Eppendorf tubes, showing successful detection of ascorbic acid in fruit juice samples in the linear range of the proposed sensor.

Fig. 8. For this purpose, fruit juices were used as real samples. The sensor demonstrated the ability to detect the analyte both qualitatively and quantitatively within its linear range. In samples where the concentration of the analyte was higher than that of the linear range of the proposed sensors, the real samples were strategically diluted and processed for further analysis.

4 Conclusion

In conclusion, a new nanocomposite of Ag–ZnO@HAp was successfully synthesized *via* the calcination method. Advanced spectroscopic techniques and morphological studies confirmed the desired synthesis. The synthesized nanocomposite was used as a peroxidase mimic enzyme that catalyzed the oxidation of TMB in the presence of hydrogen peroxide. The synthesized platform successfully detected ascorbic acid with a visible colorimetric change from blue-green to transparent, which was correspondingly confirmed using a UV-visible spectrophotometer. Various parameters affecting the sensor performance, such as the amount of the nanozyme, concentrations of TMB and hydrogen peroxide, and incubation time, were optimized. The sensor system under optimized conditions demonstrated a linear range of 5–85 μM, with a low limit of detection (0.5 μM) and a limit of quantification (1.6 μM). Interference studies confirmed the selectivity of the synthesized nanozyme. Real sample applications in fruit juices confirmed that the synthesized platform can be successfully used for real samples. The synthesized sensor can potentially be used for a wide range of applications, such as the food industry, pharmaceuticals, and health care monitoring, as a low-cost, easy-to-use, simple-to-observe platform.

Author contributions

Amir Badshah, Umar Nishan, and Wei Sun conceived the idea, supervised the work, and analyzed the data. Hasib Ullah, Xiaoping Zhang, Ijaz Ahmad, Imran Rabbani, and Khaled Fahmi Fawy performed the experiments and wrote the initial draft of the manuscript. Hasib Ullah, Umar Nishan, Wei Sun, and Amir Badshah worked on validation, visualization, and data curation. Umar Nishan and Amir Badshah worked on funding acquisition, project administration, and resources, and critically evaluated the manuscript. All the authors read and approved the final version of the manuscript.

Conflicts of interest

The authors declare no conflict of interest.

Data availability

The manuscript contains the majority of the data generated in the current work. Any additional information that may be required can be requested from the corresponding author on a reasonable basis.

Acknowledgements

The authors extend their appreciation to the Deanship of Research and Graduate Studies at King Khalid University, Saudi Arabia, through Large Research Project under grant number RGP-2/682/46. The work is also supported by Open Foundation of Hainan International Joint Research Center of Marine Advanced Photoelectric Functional Materials (2024MAPFM01).

References

1 Y. Di, J. Zheng, Y. Zhao, Z. Yang, C. Xie, J. Yu, *et al.*, Colorimetric/photothermal dual-mode sensing detection of ascorbic acid based on a Ag [i] ion/3, 3′, 5, 5′-tetramethylbenzidine (TMB) system, *RSC Adv.*, 2022, **12**, 36012–36017.
2 H. Guan, B. Han, D. Gong, Y. Song, B. Liu and N. Zhang, Colorimetric sensing for ascorbic acid based on peroxidase-like of GoldMag nanocomposites, *Spectrochim. Acta, Part A*, 2019, **222**, 117277.
3 C. Offor, P. U. Okechukwu and U. A. Esther, Determination of ascorbic acid contents of fruits and vegetables, *Int. J. Pharm. Med. Sci.*, 2015, **5**, 1–3.
4 K. Jiang, K. Tang, H. Liu, H. Xu, Z. Ye and Z. Chen, Ascorbic acid supplements and kidney stones incidence among men and women: A systematic review and meta-analysis, *Urol. J.*, 2019, **16**, 115–120.
5 Z. Zhang, X. Han, L. Wang, B. Wang, Y. Huang, M. Ahmad, *et al.*, Trimetallic ZIFs-derived nanoarchitecture for portable wireless electrochemical determination of chlorogenic acid in natural medicine and food samples, *Microchem. J.*, 2024, **207**, 111877.
6 L. Wang, X. Li, Y. Ai, X. Han, M. Ahmad, X. Zhang, *et al.*, Fabrication of graphitic carbon nitride and black phosphorene composite based electrochemical sensor and application for sensitive determination of quercetin, *Microchem. J.*, 2024, **205**, 111190.

7 M. Rong, L. Lin, X. Song, Y. Wang, Y. Zhong, J. Yan, *et al.*, Fluorescence sensing of chromium (VI) and ascorbic acid using graphitic carbon nitride nanosheets as a fluorescent "switch", *Biosens. Bioelectron.*, 2015, **68**, 210–217.
8 M. Szultka, M. Buszewska-Forajta, R. Kaliszan and B. Buszewski, Determination of ascorbic acid and its degradation products by high-performance liquid chromatography-triple quadrupole mass spectrometry, *Electrophoresis*, 2014, **35**, 585–592.
9 P. He, Y. Niu, Z.-h. Mei, J.-f. Bao and X.-m. Sun, Measurement of ascorbic acid in single rat peritoneal mast cells using capillary electrophoresis with electrochemical detection, *J. Chromatogr. B*, 2010, **878**, 1093–1097.
10 M. Asad, N. Muhammad, N. Khan, M. Shah, M. Khan, M. Khan, *et al.*, Colorimetric acetone sensor based on ionic liquid functionalized drug-mediated silver nanostructures, *J. Pharm. Biomed. Anal.*, 2022, **221**, 115043.
11 J. Xie, X. Zhang, H. Wang, H. Zheng and Y. Huang, Analytical and environmental applications of nanoparticles as enzyme mimetics, *TrAC, Trends Anal. Chem.*, 2012, **39**, 114–129.
12 H. Wei and E. Wang, Nanomaterials with enzyme-like characteristics (nanozymes): next-generation artificial enzymes, *Chem. Soc. Rev.*, 2013, **42**, 6060–6093.
13 Q. Niu, J. Zheng, L. Liu, J. Xu, H. Alsulami, M. A. Kutbi, *et al.*, Nanostructured MnO2 nanosheets grown on nickel foam: an efficient and readily recyclable 3D artificial oxidase for the colorimetric detection of ascorbic acid, *New J. Chem.*, 2020, **44**, 11959–11964.
14 X. Zheng, Q. Lian, L. Zhou, Y. Jiang and J. Gao, Peroxidase mimicking of binary polyacrylonitrile-CuO nanoflowers and the application in colorimetric detection of H2O2 and ascorbic acid, *ACS Sustain. Chem. Eng.*, 2021, **9**, 7030–7043.
15 U. Nishan, N. Jabeen, A. Badshah, N. Muhammad, M. Shah, I. Ullah, *et al.*, Nanozyme-based sensing of dopamine using cobalt-doped hydroxyapatite nanocomposite from waste bones, *Front. Bioeng. Biotechnol.*, 2024, **12**, 1364700.
16 N. Alizadeh and A. Salimi, Facile synthesis of Fe-doped hydroxyapatite nanoparticles from waste coal ash: fabrication of a portable sensor for the sensitive and selective colorimetric detection of hydrogen sulfide, *ACS Omega*, 2022, **7**, 42865–42871.
17 Y. Chengyuan, Y. Zhang and C. Jing, Molybdenum oxide supported on hydroxyapatite-encapsulated γ-Fe2O3: a novel magnetically recyclable catalyst for olefin epoxidation, *Chin. J. Catal.*, 2011, **32**, 1166–1172.
18 M. Sadat-Shojai, M.-T. Khorasani, E. Dinpanah-Khoshdargi and A. Jamshidi, Synthesis methods for nanosized hydroxyapatite with diverse structures, *Acta Biomater.*, 2013, **9**, 7591–7621.
19 T. Varadavenkatesan, R. Vinayagam, S. Pai, B. Kathirvel, A. Pugazhendhi and R. Selvaraj, Synthesis, biological and environmental applications of hydroxyapatite and its composites with organic and inorganic coatings, *Prog. Org. Coat.*, 2021, **151**, 106056.
20 D. Choi, K. G. Marra and P. N. Kumta, Chemical synthesis of hydroxyapatite/poly (ε-caprolactone) composites, *Mater. Res. Bull.*, 2004, **39**, 417–432.
21 R. N. Granito, A. C. M. Renno, H. Yamamura, M. C. de Almeida, P. L. M. Ruiz and D. A. Ribeiro, Hydroxyapatite from fish for bone tissue engineering: A promising approach, *Int. J. Mol. Cell. Med.*, 2018, **7**, 80.
22 W. Khoo, F. Nor, H. Ardhyananta and D. Kurniawan, Preparation of natural hydroxyapatite from bovine femur bones using calcination at various temperatures, *Procedia Manuf.*, 2015, **2**, 196–201.
23 S. Ibrahim, J. Iqbal, M. Shah, W. Sun, M. Asad, M. Ullah, *et al.*, From Waste to Sensor: Facile Synthesis of a Copper-Doped Hydroxyapatite Nanocomposite as a Colorimetric Sensing Platform for Uric Acid, *ChemistrySelect*, 2024, **9**, e202402879.
24 S. Mondal, M. E. D. A. Reyes and U. Pal, Plasmon induced enhanced photocatalytic activity of gold loaded hydroxyapatite nanoparticles for methylene blue degradation under visible light, *RSC Adv.*, 2017, **7**, 8633–8645.
25 A. Khaliq, R. Nazir, M. Khan, A. Rahim, M. Asad, M. Shah, *et al.*, Co-doped CeO_2/activated C nanocomposite functionalized with ionic liquid for colorimetric biosensing of H_2O_2 via peroxidase mimicking, *Molecules*, 2023, **28**, 3325.
26 R. Ullah, M. Soylak, M. Asad, M. Khan, M. Shah, N. Khan, *et al.*, Manganese oxide-doped graphitic carbon nitride-based 2D material as nanozyme for the colorimetric sensing of ascorbic acid, *Sens. Actuators, A*, 2024, **380**, 115995.
27 L. Chang, Y. Feng, B. Wang, X. Huang, D.-P. Yang and Y. Lu, Dual functional oyster shell-derived Ag/ZnO/$CaCO_3$ nanocomposites with enhanced catalytic and antibacterial activities for water purification, *RSC Adv.*, 2019, **9**, 41336–41344.
28 M. T. Alula and N. R. Hendricks-Leukes, Silver nanoparticles loaded carbon-magnetic nanocomposites: A nanozyme for colorimetric detection of dopamine, *Spectrochim. Acta, Part A*, 2024, **322**, 124830.
29 H. Lyu, X. Zhao, X. Yao, W. Chen, Z. Liu, L. Gao, *et al.*, 3, 4: 9, 10-perylene tetracarboxylic acid-modified zinc ferrite with the enhanced peroxidase activity for sensing of ascorbic acid, *Colloids Surf., A*, 2020, **586**, 124250.
30 H. Chen, C. Yuan, X. Yang, X. Cheng, A. A. Elzatahry, A. Alghamdi, *et al.*, Hollow mesoporous carbon nanospheres loaded with Pt nanoparticles for colorimetric detection of ascorbic acid and glucose, *ACS Appl. Nano Mater.*, 2020, **3**, 4586–4598.
31 W. Lu, J. Zhang, N. Li, Z. You, Z. Feng, V. Natarajan, *et al.*, Co_3O_4@ β-cyclodextrin with synergistic peroxidase-mimicking performance as a signal magnification approach for colorimetric determination of ascorbic acid, *Sens. Actuators, B*, 2020, **303**, 127106.
32 T. Wu, Z. Ma, P. Li, M. Liu, X. Liu, H. Li, *et al.*, Colorimetric detection of ascorbic acid and alkaline phosphatase activity based on the novel oxidase mimetic of Fe–Co bimetallic alloy encapsulated porous carbon nanocages, *Talanta*, 2019, **202**, 354–361.
33 Y. Han, L. Luo, L. Zhang, Y. Kang, H. Sun, J. Dan, *et al.*, Oxidase-like Fe–Mn bimetallic nanozymes for colorimetric detection of ascorbic acid in kiwi fruit, *Lwt*, 2022, **154**, 112821.